Electronic band structure of zinc blende

S. R. Barman,* S.-A. Ding,† G. Neuhold,‡ and K. Horn
Fritz-Haber-Institut der Max-Planck-Gesellschaft, D-14195 Berlin, Germany

D. Wolfframm and D. A. Evans
Department of Physics, University of Wales, Penglais, Aberystwyth, United Kingdom

(Received 23 January 1998; revised manuscript received 27 April 1998)

The electronic bulk and surface band structure of cubic zinc sulphide (''zinc blende'') has been studied by angle-resolved photoelectron spectroscopy using synchrotron radiation. The s-p derived bands along the Γ-K-X high-symmetry direction have been determined, and the region of the Zn $3d$ line has been examined. Spectra at fixed photon energy and variation of polar electron emission angle were used to determine the dispersion of the surface states along the $\bar{\Gamma}$-$\bar{X}$ within the surface Brillouin zone. The experimental data for bulk and surface bands are compared with results of a recent density-functional calculation, which includes the interaction between the s-p and the cation d-derived states. [S0163-1829(98)09635-0]

I. INTRODUCTION

The electronic structure of II-VI semiconductors has received renewed interest in view of their applications in novel optoelectronic devices.[1] Epitaxial growth of II-VI materials of high quality is now routinely achieved, and optoelectronic devices such as light emitting diodes and lasers based on the ZnS/ZnSe class of materials have been demonstrated.[2] However, a detailed study of the electronic band structure of ZnS using angle-resolved photoemission has not been published to date. Such data are useful for determining the trends in band dispersions and the energies of the shallow core levels across the II-VI and III-V families of materials. It is also useful to compare the electronic structure of those II-VI materials that occur both in the wurtzite and the (in some cases metastable) cubic conformation.[3–6] These are similar in that both have a tetragonal coordination with their nearest neighbors, and nearly identical distances with their second nearest neighbors. This is also true for ZnS, since growth on hexagonal ZnS results in wurtzite layers, whereas on cubic substrates the cubic (zinc blende or sphalerite) phase results.[7]

Here we report on a band-structure investigation of cubic ZnS by means of angle-resolved photoelectron spectroscopy. Growth of ZnS on GaAs results in a strained layer in view of the lattice mismatch between these materials, which may be removed by a sequence of ZnS_xSe_{1-x} buffer layers. We have circumvented this complication by growing epitaxial layers on GaP(110), since the lattice mismatch between GaP and cubic ZnS is only about 0.7%. Our previous study of the epitaxial growth of ZnS on GaP(110) has shown that layers of good crystalline quality can be grown this way. Moreover, ZnS crystals of sufficient size, and with a carrier concentration high enough for photoemission experiments, are not available.

A study of the valence-band structure of II-VI semiconductors is timely since advances have recently been made in the theoretical description of their electronic structure. The valence bands of the II-VI materials differ in one important aspect from that of the III-V group of semiconductors, in that the cation d states are much closer in energy to the upper valence bands, and are thus expected to have a much stronger interaction with these. In fact, recent quasiparticle calculations for CdS using the GW approximation have shown that the full cationic shell with main quantum number $n=4$ must be taken into account in order to provide a description that shows good agreement with experiment.[8] This is particularly evident in the energy of the cation d level, which may show deviations of up to 4 eV from the experimentally determined binding energy if such corrections are not taken into account. Our present study extends this comparison to cubic ZnS. Pollmann and co-workers have recently obtained an equally satisfactory description of the d-p interaction through their self-interaction and relaxation-corrected pseudopotentials (SIRC-PP), which have been used to study the electronic structure of many II-VI compound semiconductors,[9] among them cubic ZnS.

II. EXPERIMENT

All experiments were carried out in an ultrahigh-vacuum photoelectron spectrometer with a base pressure of about 8×10^{-11} mbar, equipped with a high-resolution angle-resolving electron energy analyzer (HA 50 from VSW Ltd. UK, and ADES 400 from Vacuum Generators, UK), a cleavage tool, sample load lock, temperature-controlled manipulator that allowed cooling and heating of the sample, molecular-beam epitaxy (MBE) cells, and a low-energy electron diffraction (LEED) optics (Omicron GmbH, Germany) for the study of overlayer crystallinity. Crystals of GaP (MCP Ltd., UK), with a carrier concentration of 3×10^{17} cm^{-3}, were oriented and cut to be cleaved using the double-wedge technique. ZnS with 99.9999% purity (Crystal GmbH, Berlin) was deposited from a water-cooled MBE cell at temperatures of around 650 °C, leading to growth rates of about 0.1–0.5 nm/min. Soft-x-ray photons from the BESSY (Berliner Elektronen-Speicherring-Gesellschaft für Synchrotronstrahlung mbH) storage ring were dispersed by the TGM 4 toroidal grating monochromator. The system provided an overall resolution of about 70–150 meV for photon energies between 12.5 and 100 eV. Overlayers were grown, as previ-

 © 1998 The American Physical Society

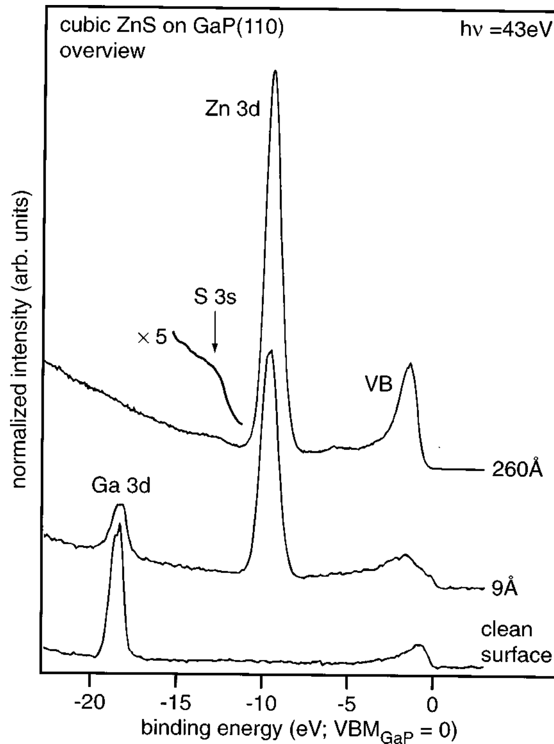

FIG. 1. Valence level spectra for the clean GaP(110) surface and two depositions of ZnS as indicated, recorded in normal emission at a photon energy of 43 eV. Note the change in appearance of the features near the valence-band maximum (VBM), and the shift of the VBM as the ZnS layer builds up.

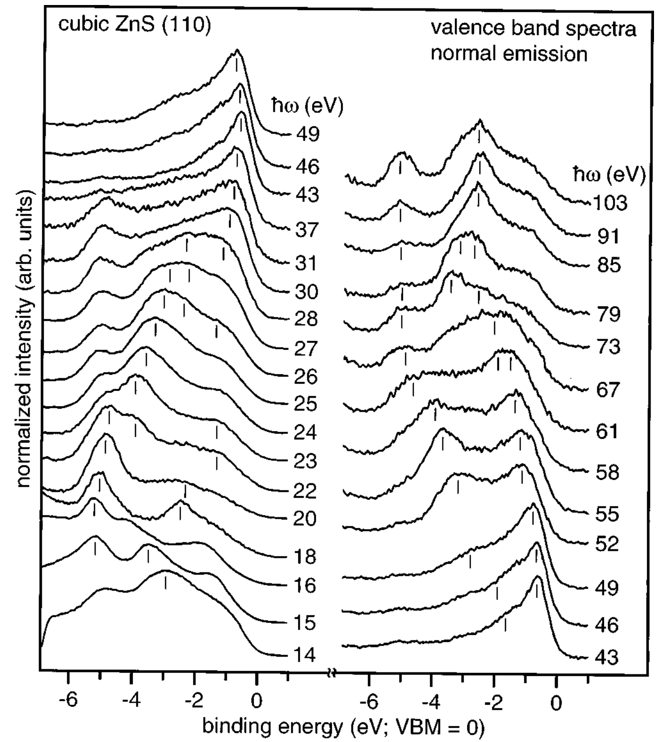

FIG. 2. Series of valence-band spectra from a 260-Å-thick ZnS(110) layer, recorded in normal emission for photon energies from 14 to 103 eV. Note the shift of some features with photon energy, indicative of **k**-conserving transitions.

ously described,[10] on several different substrates in order to establish the optimal growth temperature of 100 °C, characterized by a minimum amount of interface reaction as judged from the Ga 3d core levels, and the quality of the LEED diffraction pattern. Photoemission spectra were recorded with the light impinging onto the sample at an angle of incidence of 45°, with the plane of polarization of the linearly polarized light parallel to the [100] azimuth.

III. RESULTS AND DISCUSSION

A. Bulk band structure

An overview of the band structure of cubic ZnS can be obtained from the set of normal-emission spectra shown for increasing thickness in Fig. 1, recorded at a photon energy of 43 eV. The bottom spectrum shows the features of the clean GaP(110) surface, with emission concentrated near the valence-band maximum (VBM), and the intense Ga 3d core-level emission at a binding energy of 18.5 eV with respect to the VBM of GaP. Upon depositing 9 Å ZnS, the Zn 3d emission emerges, and the valence band shows an extra peak at about 2 eV below the VBM. At a layer thickness of 93 Å, the ZnS features dominate the spectrum, with the Zn 3d peak more intense. Finally, at 260 Å ZnS, smaller features in the VB can be seen, and a weak feature below the Zn 3d line is observed, which we ascribe to the sulfur 3s level, as discussed later in the text. Our determination of the valence-band dispersion $E(\mathbf{k})$ of different bands is based on the well-known free-electron final-state model, where electron momentum $k_\perp$ along the high-symmetry direction normal to the crystal surface [Γ-K-X for the present case of a (110) surface] is determined on the basis of the free-electron relation

$$k_\perp = \sqrt{2m/\hbar^2}\sqrt{(E-V_0)}, \tag{1}$$

where V_0 is the inner potential. This is the only free parameter in this model, and is adjusted to give identical initial band energies for specific transitions to different final-state branches.

Normal-emission spectra for a 260 Å ZnS film, taken over a wide range of photon energies (14–103 eV), are shown in Fig. 2. All features except the lowest binding-energy peak at about 5 eV below the VBM exhibit dispersion with photon energy, and this is a clear sign of bandlike behavior of the initial states. This is particularly evident in the second peak from the VBM at photon energies of 14, 15, and 16 eV, and the same peak, reversing its movement towards the VBM, at photon energies between 22 and 27 eV. Another set of clearly dispersing peaks is the second peak again between 49 and 58 eV photon energy. What is less obvious upon first inspection is the shift in the peak near the VBM, for example, between 31 and 49 eV. Finally, a clear sign for the dominance of direct i.e., **k**-conserving transitions, is the narrowing of the entire spectrum, and the binding-energy minimum of the leading peak, at a photon energy of 43 eV, suggesting that transitions at a critical point are reached here.

It is well known that the band structures of the cubic III-V and II-VI semiconductors exhibit several similarities, and thus the general course of the bands is known: at the Γ point, all three p-like bands coalesce (except for spin-orbit interaction, which causes the bands to split). The bands disperse

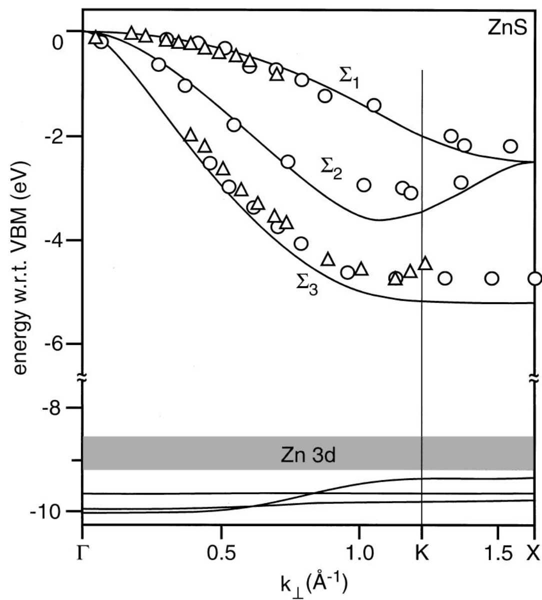

FIG. 3. Experimental band structure of cubic ZnS along the Γ-*K*-*X* direction; a constant offset of 0.65 eV is used for the peak positions with respect to Fig. 2. The lines are from the density-functional band-structure calculation by Vogel *et al.* (Ref. 9) discussed in the text.

down towards *K* and *X*, with the top two bands becoming degenerate at *X*. In order to derive an experimental band structure, one needs to determine peak positions that correspond to the initial-state energies. For clearly separated peaks of a reasonable shape, this is straightforward, but there are cases where only a shoulder can be distinguished. In the absence of available calculations of the photoelectron spectrum, or a suitable model function for the peak shape of valence transitions, we use clearly distinguishable peaks or shoulders and also take into account situations where peaks become broader with photon energy. These peaks are then translated into points in an $E(\mathbf{k})$ diagram on the basis of values calculated for **k** from Eq. (1), using an inner potential of 6.5 eV. This diagram, where **k** is given in Å^{-1}, in the range from Γ through *K* and *X*, is shown for the region of the valence bands and Zn 3*d* levels in Fig. 3. Here the data are plotted such that the transitions at the lowest binding energy are set equal to the valence-band maximum, which involves a rigid shift of 0.65 eV of all bands when compared with the plot of the raw spectra in Fig. 2. Also shown is a calculated band structure for the valence bands, based on the density-functional theory (DFT) calculation using the self-interaction and relaxation-corrected pseudopotentials of Vogel *et al.*[9] (solid lines). The three bands expected from the general shape of the band structure are clearly seen in the experimental data, and they closely follow the dispersions predicted by the calculation. The range of photon energies accessible here permits the detection of direct transitions from the Γ point out to *K* and beyond *X*, covering this branch of the band structure twice, such that we have two independent data sets, a fact that puts the determination of the inner potential, and the shape of the bands, on a solid foundation. For the region between *K* and *X*, we note that the lowest band does not disperse much, as expected. For the first and second (Σ_1 and Σ_2) bands, it is clear from the data points that they are degenerate at *X*, as expected on symmetry grounds.

There are several calculations of the cubic ZnS band structure, from the early empirical pseudopotential ones up to the present density-functional schemes, which use the local-density approximation (LDA) for the inclusion of correlation and exchange. Though the latter are *ab initio* calculations, they are known to be subject to two shortcomings. First, they generally underestimate the size of the fundamental band gap, by up to 90% in some cases [ZnO (Ref. 9)], since the eigenvalues of the Kohn-Sham equations have only a physical meaning for the highest occupied states. Second, the DFT-LDA calculations fail to correctly describe strongly localized corelike *d* states and thus underestimate their binding energies. The reason for this lies in an unphysical self-interaction, and in a neglect of the electronic relaxation in the standard LDA calculation for such states. This moves the *d* states much closer towards the topmost *p* states, artificially enlarging their mutual interactions and negatively affecting the dispersion of the *p* states, by shifting them much closer to the conduction bands.

The problem of *d*-*p* interaction is not very important for III-V semiconductors, where the *d* states are about 10–12 eV below the *p* states. However, in the present case of the II-VI compounds, the *d* states of Zn, Cd, and Hg are within about 4–5 eV of the *p* states. One way to overcome this problem is to perform quasiparticle band-structure calculations based on the *GW* approximation, including the semicore electrons explicitly. Such calculations have been carried out for cubic CdS and ZnSe. However, they are very time-consuming even for bulk crystals, and forbidding for surface or interface calculations. Pollmann and co-workers have recently devised an alternative way to deal with this situation, by introducing self-interaction corrections (SIC) into the standard LDA calculations. They have also devised a variant of this scheme by which even electronic relaxation is taken into account (self-interaction and relaxation corrections, SIRC). This work is partly based on previous work by Zunger[11] and Rieger and Vogl.[12] Here, new pseudopotentials are constructed that take into account self-interaction and relaxation in the constituent *atoms*, by reference to the atomic Δ-self-consistent-field approach pioneered by Hedin and Johansson.[13] The new pseudopotentials can then be used in a standard LDA code. A strong justification for taking atomic relaxation as a basis for a solid-state calculation is provided by the observation that the difference between experimental and theoretical binding energies of the cation *d* states is roughly constant for the II-VI semiconductors, irrespective of lattice constant and whether zinc-blende or wurtzite lattices are taken into account.

In a previous publication, we have performed an experimental determination of the valence-band structure of cubic CdSe, and have compared our results with a theoretical band structure based on the SIC and SIRC approach. As well as obtaining good agreement for the upper valence bands, it was found that the binding energy of the Cd 4*d* states is well represented by the calculations. The calculations predict a sizable dispersion in these states, and by comparing a calculated density of states in this region with an experimental spectrum, we were able to explain a shoulder peak on the Cd

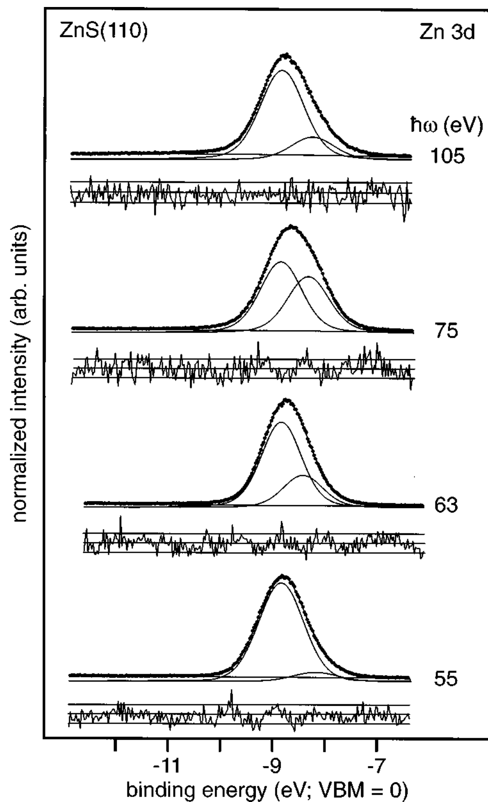

FIG. 4. Set of spectra for the region of the Zn $3d$ peak, with a Gaussian fit to the line shape discussed in the text. The lines below each spectrum indicate the residuum.

$3d$ peak in terms of a strongly dispersing band, in contrast to previous publications that had assigned this feature to emission from the Se $4s$ band.

In line with our expectations, a comparison between the SIRC calculations and our experimental data for the binding energy of the Zn $3d$ band in cubic ZnS yields an equally gratifying result as in the case of cubic CdSe. This is shown in the lower part of the band structure of Fig. 3, and in Fig. 4, where four spectra of the Zn $3d$ region are shown, recorded at different photon energies in normal emission. The experimental binding energy of 8.9 eV below the VBM compares well with the calculated value of 9.4 eV.[9] There is no clear indication for Zn $3d$ dispersion in the raw data, such as shoulder peaks, in the spectra of Fig. 4. In order to distinguish changes in the line shape, we have performed a set of Gaussian fits to these spectra. The spectrum for $\hbar\omega = 55$ eV can be fitted with one dominating Gaussian and a small contribution to take account of a small asymmetry towards lower binding energies. The main Gaussian has a constant full width at half maximum (FWHM) for a fit of all spectra, which is reasonable since the linewidth (about 1.5 eV) is much larger than the experimental resolution, which increases from about 100 to about 180 meV over the range of photon energies used for the spectra in Fig. 4. We note that the second Gaussian becomes increasingly important for a reasonable fit for $\hbar\omega = 63$ and 75 eV, but decreases in intensity beyond this energy (see the spectrum for $\hbar\omega = 105$ eV); in fact, the spectrum at 75 eV has a markedly broader peak. We regard this as an indication that the contributions from the Zn $3d$ band (five bands in all at an arbitrary point in **k** space) exhibit some degree of dispersion, which makes the peak appear broader and more asymmetric in the second and third spectrum from the bottom. This view is supported by the observation that the peak in fact becomes narrower at 105 eV, where it should broaden if the instrumental resolution, which is lowest here, were responsible for this effect. A further determination of the dispersion of the Zn $3d$ levels cannot be performed in this manner since the intrinsic linewidth is too large for an assignment in terms of separate dispersing bands. The identification of the anion s level with the small peak about 3.5 eV below the Zn $3d$ peak (shown enlarged in Fig. 1) precludes any involvement of this level in the Zn $3d$ peak group. It also gives a graphic comparison of intensities of these two peaks. The assignment of this small feature to the sulfur $3s$ peak is supported by the valence-band photoemission data taken with high (1253.6 eV) photon energy,[14] which shows this peak much more clearly since the cross-section difference for the Zn $3d$ and S $3s$ levels decreases at higher photon energies. The SIRC calculations also located the center of gravity of the sulfur $3s$ band at about 3 eV below the Zn $3d$ energy.

B. Emission from surface states

An experimental determination of the bulk band structure of III-V and II-VI compound semiconductors by means of photoemission is facilitated by the fact that the spectra are only moderately affected by surface-state emission. This a well-known problem in the more heavily reconstructed low index surfaces of the elemental semiconductors,[15] the photoemission spectrum of which is largely dominated by surface-state emission, masking the bulk band transitions. The situation is less complicated on the (110) surfaces of the zinc-blende-type semiconductors, where the surface is only modified by a mild atomic rearrangement in the bond-angle rotation relaxation and leads to a redistribution of charge from the cations to the anions. This causes the anion dangling-bond surface state to become fully occupied, moving its energy into the valence band, while the cation dangling-bond state becomes empty, moving into the conduction band.[16] The fundamental band gap is thus devoid of surface states. Surface band-structure calculations predict a number of surface-related features for the zinc-blende (110) surfaces, for example for GaAs. A large body of data has been collected on the dispersion of occupied and unoccupied dangling-bond states on these surfaces.[17] A strong surface-related feature that is found on all (110) surfaces of the III-V compound semiconductors, near the VBM at the center of the surface Brillouin zone, has been related to the anion dangling-bond state. Generally, this surface state is observed a few hundred meV below the VBM at the center $\bar{\Gamma}$ of the surface Brillouin zone (BZ) [with the possible exception of GaSb (110) (Ref. 18)], and disperses to higher binding energies for increasing values of the parallel component of the electron wave vector $k_{\parallel}$ towards the $\bar{X}$ point at the surface BZ boundary. Such a trend is indeed observed in the leading peak in the series of spectra shown in Fig. 5, recorded at a photon energy of 43 eV for varying angles along the [001], i.e., $\bar{\Gamma}$-$\bar{X}$ azimuth. The trend in the peak dispersion is found to reverse beyond the surface Brillouin-zone boundary, with the energy of the leading peak almost reaching the initial

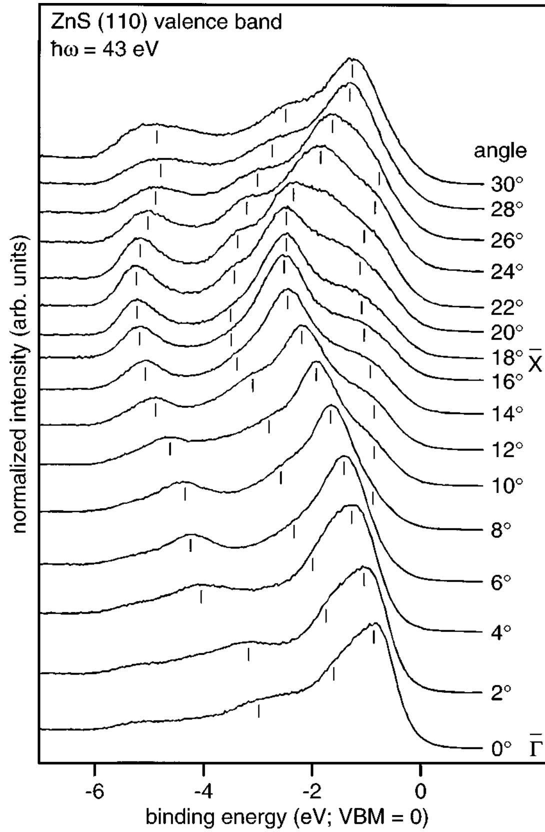

FIG. 5. Set of spectra from a 260-Å-thick ZnS(110) layer, recorded at a photon energy of 43 eV for different values of $k_\parallel$ along the $\bar{\Gamma}$-$\bar{X}$ direction of the surface Brillouin zone. The intense peak near the VBM exhibits a strong dispersion away from the VBM and is seen to reverse this trend beyond the Brillouin-zone boundary at $\bar{X}$ ($k_\parallel = 0.82$ Å^{-1}).

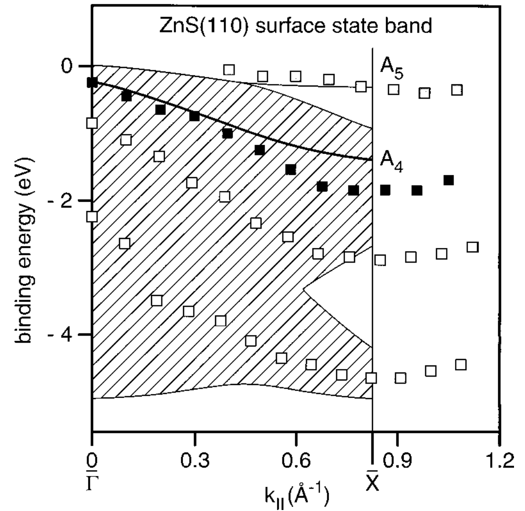

FIG. 6. Surface band structure of ZnS along the $\bar{\Gamma}$-$\bar{X}$ direction. The data points are from an evaluation of the angle-resolved spectra in Fig. 5 (see text); a constant offset of 0.65 eV is used for the peak positions with respect to Fig. 5. The lines are from the SIRC-PP calculation of the ZnS(110) surface bands, where the hatched area indicates the region where bulk bands exist.

energy at $\bar{\Gamma}$ (polar angle $\Theta = 0°$) as $k_\parallel$ comes close to the $\bar{\Gamma}$ point of the second surface Brillouin zone. This demonstrates that the leading peak in fact is surface derived, since the surface Brillouin zone of the cubic (110) surface, when projected onto the bulk Brillouin zone, is smaller than the latter, such that a bulk-derived band cannot exhibit a reversal of dispersion at this point (see Fig. A1 in Ref. 19). An interesting feature is the broad emission above the strongly dispersing surface state, which appears as a shoulder close to the VBM for angles from 10° to 24°. This emission occurs in a region where no bulk bands exist according to the projected bulk band structure (Fig. 6), and is therefore also surface-related; however, the possibility that it might be due to umklapp processes involving bulk bands cannot be ruled out. The origin of this state is discussed in comparison to surface band-structure calculations below.

Two other features in the spectrum appear to have a similar behavior. These are a shoulder peak, seen in normal emission at about 1.5 eV binding energy with respect to the VBM, which comes out quite clearly in the spectrum at higher $k_\parallel$, and a peak at about 2.8 eV below the VBM, which at higher values of $k_\parallel$ moves towards the stationary peak at 5.3 eV, derived from the large density of states of the lowest band between the K and X points of the bulk Brillouin zone. This third dispersing peak is also seen to move back towards the VBM beyond the zone boundary. The photon energy of 43 eV was chosen for this experiment since it has been shown[20] that surface-state photoemission intensity exhibits a strongly oscillatory behavior. It becomes strongly enhanced for photon energies at which bulk bands close in energy undergo direct transitions. The dangling-bond surface state in ZnS is closest in energy to the bands at the Γ point of the bulk Brillouin zone, and thus it becomes enhanced in intensity at those photon energies where direct transitions between states at Γ occur; a similar behavior in surface-state emission from compound semiconductors was previously found in InP(110).[21] Thus, the observation of strong emission from a state that is clearly identified with a surface state from its dispersion trend with $k_\parallel$, is an independent confirmation of the assignment of transitions near Γ from the free-electron final-state model above.

The dispersion of the surface-related peaks in the set of spectra in Fig. 5 is displayed in Fig. 6, between $\bar{\Gamma}$ and $\bar{X}$, by filled, gray, and open squares; again, a rigid shift of 0.65 eV towards lower binding energy was carried out with respect to the plot in Fig. 5. The dispersion of the leading peak in normal emission is shown by filled squares, while the shoulder that is clearly seen at the lower-binding-energy side of the leading peak is shown by gray squares. The weaker higher-binding-energy features in the spectra of Fig. 5 are shown as open squares. Also shown is the region of the projected bulk bands and the dispersion surface-related features derived from the SIRC-PP calculation of Vogel *et al.*[22] The calculations, which predict *two* surface bands labeled A_4 and A_5 close to the VBM, differ from the body of theoretical data that has been assembled on the surface band structure of the III-V materials, which only predict *one* surface state. This is expected to occur within a simple picture of broken bonds at the surface, in contrast to the calculations for the III-V semiconductors. From calculated charge-density maps, Vogel *et al.* identified the strongly dispersing A_4 state with the in-plane surface bond, while the rather weakly dispersing

A_5 is assigned to the dangling-bond state. These two states are quite different in their dispersion across the surface Brillouin zone; the dangling-bond state exhibits only a small dispersion (about 0.2 eV), while the in-plane bond state has a large (1 eV) dispersion. While one may argue that the experimental data in Figs. 5 and 6 show good agreement with the SIRC-PP calculations, such that the leading peak would be assigned to the A_4 in-plane surface bond (filled squares) and the lower binding-energy shoulder to the A_5 dangling bond (gray squares), the present data cannot be regarded as proof for the rather unexpected result of the SIRC-PP calculations, since this differs from a large body of theoretical data for similar III-V compound semiconductor surfaces. This aspect merits further investigation, in particular from a theoretical point of view where a comparison between these different approaches for a well-studied system would be most interesting. The two features found at higher binding energies are located in the region of the projected bulk bands, such that they must be ascribed to surface resonances. Such resonances are often difficult to identify, although they have been predicted to exist on many (110) surfaces of III-V compound semiconductors (see, for example, Ref. 17 or the data collection in Ref. 23). No evidence for such surface-derived states have been found in this region in the SIRC-PP calculations, however.

In summary, we have used photoelectron spectroscopy for a study of the band structure of cubic ZnS along the Γ-K-X line, and found clear evidence for k-conserving transitions. These have been used to determine the band dispersion on the basis of a free-electron final-state model. The dispersion of the surface-related peaks in the spectra has been mapped along the $\bar{\Gamma}$-$\bar{X}$ direction in the surface Brillouin zone, and was compared with a surface band-structure calculation.

ACKNOWLEDGMENTS

This work was supported by the Bundesministerium für Bildung, Forschung, und Technologie under Grant No. 05 622 OLA. D.A.E. acknowledges funding by the European Community through the HCM-LSI program. We acknowledge the help of H. Haak with technical preparations.

*Present address: Inter University Consortium, University Campus, Khandwa Road, Indore, India.
†Present address: LASST, University of Maine, Orono, ME 04469.
‡Present address: Dresdner Bank AG, D-60301 Frankfurt, Germany.

[1] M. Jain, in *II-VI Semiconductor Compounds* (World Scientific, Singapore, 1993).
[2] M. A. Haase, J. Qiu, J. M. DePuydt, and H. Cheng, Appl. Phys. Lett. **59**, 1272 (1991).
[3] W. G. Wilke and K. Horn, J. Vac. Sci. Technol. B **6**, 1211 (1988).
[4] W. G. Wilke, R. Seedorf, and K. Horn, J. Vac. Sci. Technol. B **7**, 807 (1989).
[5] P. Hofmann, K. Horn, A. M. Bradshaw, D. Fuchs, M. Cardona, and R. L. Johnson, Phys. Rev. B **47**, 1639 (1993).
[6] K. O. M. Magnusson, G. Neuhold, D. A. E. Evans, and K. Horn, Phys. Rev. B **57**, 8945 (1998).
[7] K. Lark-Horowitz and S. E. Madigan, Phys. Rev. **44**, 320 (1933).
[8] M. Rohlfing, P. Krüger, and J. Pollmann, Phys. Rev. Lett. **75**, 3489 (1995).
[9] D. Vogel, P. Krüger, and J. Pollmann, Phys. Rev. B **54**, 5495 (1996).
[10] D. Wolfframm, P. Bailey, D. A. Evans, G. Neuhold, and K. Horn, J. Vac. Sci. Technol. A **14**, 844 (1996).
[11] A. Zunger, Phys. Rev. B **22**, 649 (1980).
[12] M. Rieger and P. Vogl, Phys. Rev. B **52**, 16 567 (1995).
[13] L. Hedin and A. Johansson, J. Phys. B **2**, 1336 (1969).
[14] L. Ley, R. A. Pollak, F. R. McFeely, S. P. Kowlaczyk, and D. A. Shirley, Phys. Rev. B **9**, 600 (1974).
[15] D. H. Rich, G. E. Franklin, F. M. Leibsle, T. Miller, and T. C. Chiang, Phys. Rev. B **40**, 11 804 (1989).
[16] W. Mönch, *Semiconductor Surfaces and Interfaces* (Springer-Verlag, Berlin, 1993).
[17] G. V. Hansson and R. I. G. Uhrberg, Surf. Sci. Rep. **9**, 197 (1988).
[18] R. Manzke, H. P. Barnscheidt, C. Janowitz, and M. Skibowski, Phys. Rev. Lett. **58**, 610 (1987).
[19] E. W. Plummer and W. Eberhardt, Adv. Chem. Phys. **49**, 533 (1982).
[20] S. G. Louie, P. Thiry, R. Pinchaux, Y. Petroff, D. Chandesris, and J. Lecante, Phys. Rev. Lett. **44**, 549 (1980).
[21] L. Sorba, V. Hinkel, H. U. Middelmann, and K. Horn, Phys. Rev. B **36**, 8075 (1987).
[22] D. Vogel and J. Pollmann (unpublished).
[23] *Landolt-Börnstein, Physics of Solid Surfaces*, edited by G. Chiarotti (Springer-Verlag, Berlin, 1996).